Chronology of the Middle–Upper Pliocene succession in the Strongoli area: constraints on the geological evolution of the Crotone Basin (Southern Italy)

L. CAPRARO, C. CONSOLARO, E. FORNACIARI, F. MASSARI & D. RIO

Dipartimento di Geologia, Paleontologia e Geofisica, Università di Padova, Via Giotto 1, 35137 Padova, Italy (e-mail: chiara.consolaro@unipd.it)

Abstract: The aim of this study is to reconstruct the evolution of the Strongoli area, a critical sector of the Crotone Basin (Calabria, Southern Italy), where a thick Middle–Upper Pliocene marine succession is present. The Strongoli succession shows prominent changes in the sedimentary environment that are partly forced by tectonics. Major tectonostratigraphic events have been recognized that might correlate with spreading pulses in the back-arc Tyrrhenian Sea. In particular, we demonstrate that a dramatic basinal collapse at *c*. 2.3 Ma correlates with the so-called 'Calabrian transgression' *Auctorum* and is close in age to the oceanization of the Marsili Basin.

The Strongoli area, located at the northeastern border of the late Neogene Crotone Basin, was indicated by *Roda* (1964) as a critical sector for reconstructing the tectonostratigraphic evolution of the region. The aim of this paper is to reconstruct the major geological features of the Middle–Late Pliocene succession of the Strongoli area (Figs 1 and 2). In particular, our main targets are: (1) to constrain in time and stress the regional importance of a basinal collapse event that correlates with the 'Calabrian transgression' *Auctorum* (Early Pleistocene according to Ogniben 1955); (2) to provide age control for a widespread Mid-Pliocene tectonostratigraphic event, poorly constrained so far, which corresponds to the beginning of the third sedimentary cycle of Roda (1964; Fig. 3); (3) to verify the response of the forearc stratigraphy to the dynamics of the Tyrrhenian back-arc, which can provide important clues for reconstructing the dynamics of plate interactions.

Geological and stratigraphical setting of the Crotone Basin

The Crotone forearc basin is located in the Ionian Calabria (Fig. 1), where one of the thickest and best-exposed Late Miocene to Pleistocene marine sedimentary succession of the recently uplifted Southern Italy is present. The Crotone Basin was regarded by Van Dijk (1992) as an oblique, thin-skinned strike-slip basin, created by a pull-apart between the Petilia–Rizzuto and Rossano–San Nicola NW-trending shear zones (Fig. 2) and probably detached at a depth of a few kilometres.

The stratigraphy of the Crotone Basin as established by Roda (1964) in the 1960s is still generally valid. Roda subdivided the succession into three tectonostratigraphic sequences (Fig. 3). The first sequence develops from the opening of the basin (Mid-Miocene) to intra-Messinian times, the second from late Messinian to Early Pliocene times, and the third from Mid-Pliocene to Mid-Pleistocene times. This subdivision is based on major unconformities corresponding to main reorganization events within the Crotone Basin.

Later, Van Dijk and coworkers (Van Dijk 1991, 1994; Van Dijk & Okkes 1991; Van Dijk & Scheepers 1995) proposed a model in which relationships are analysed between oceanization episodes in the Tyrrhenian Sea, active southeastward arc migration, and opening of basins in the forearc area. A long-lasting tensional regime, characterized by three major phases of subsidence and basin opening in late Tortonian, Early Pliocene and Late Pliocene times, would have been punctuated by short-lived phases of compressional deformation in the Mid-Pliocene and Mid-Pleistocene as a result of plate convergence and the end of the rollback process.

The Strongoli area: previous studies

The most prominent feature of the geological landscape of the Strongoli area is represented by a sandstone body >80 m thick and 6 km wide upon which the village of Strongoli is built (Fig. 4), extending eastwards towards the Ionian coast (Fig. 5). This sandstone body is bracketed between two mainly pelitic units that have been named and interpreted differently by Ogniben (1955) and Roda (1964), as shown in Figure 6.

Ogniben (1955) interpreted the 'Strongoli Sandstone' (hereafter SS) as the regressive unit of a Pliocene transgressive–regressive cycle, in which the underlying 'Timpa Biso Marly Clay' (TBMC)

From: MORATTI, G. & CHALOUAN, A. (eds) 2006. *Tectonics of the Western Mediterranean and North Africa*. Geological Society, London, Special Publications, **262**, 323–336.
0305-8719/06/$15.00

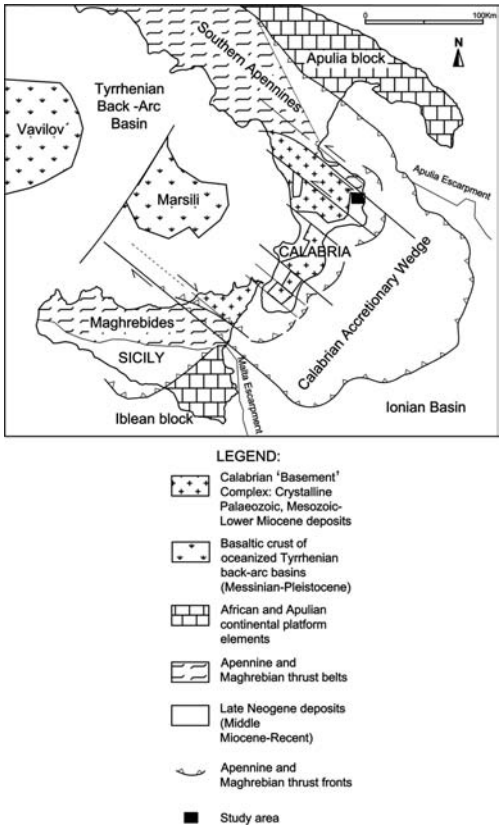

Fig. 1. Outlines of the main geological units and structural elements of southern Italy and surrounding basins (adapted from Van Dijk 1994).

would represent a transgressive portion. Likewise, the overlying 'Gigliolo Clay' (GC) would record the transgressive stage of a younger sedimentary cycle, also known as the 'Calabrian transgression' *Auctorum* (i.e. Gignoux 1913; Ruggeri & Selli 1948; Selli 1949; Ogniben 1955).

In contrast, Roda (1964) considered the TBMC and GC of Ogniben (1955) simply as component members of the Middle Pliocene–Lower Pleistocene 'Cutro Marly Clay' (CMC), whereas he regarded the SS as the record of a local sedimentary episode within the CMC with no major eustatic significance (Fig. 6). In Roda's interpretation, the offshore CMC would gradually onlap shallow-water and lagoonal units that are present in the most marginal part of the Crotone Basin (i.e. the Scandale sandstone and the Spartizzo marly clay, respectively) beginning from the base of the third tectonostratigraphic cycle (Figs 3 and 6).

In this paper, we will follow the formational terminology of Ogniben (1955) because it is more appropriate for presenting our data and more in keeping with our interpretation of the geological evolution of the Crotone Basin.

However, we could not resolve firmly the puzzling relationship between the TBMC and the underlying Murgie sandstone body (Fig. 4a), which extends west of the study area (Fig. 5). This unit was considered by Ogniben (1955) and Roda (1964) as mainly belonging to the Scandale Formation, in substantial stratigraphic continuity with the TBMC and thus belonging to the third cycle of Roda (1964). In contrast, Zecchin *et al.* (2004) correlated the Murgie body with the second cycle of Roda (1964).

Material and methods

We collected a total of about 100 samples from two sections (namely, the 'Ecce Homo' and 'Strongoli' sections) and from intervening tracts (spot samples). The integration of facies analysis with the study of foraminiferal assemblages was aimed at reconstructing the depositional environment with special reference to the formation of Mediterranean sapropel-like layers. Pollen and stable oxygen isotope studies on selected intervals provided critical information on the climatic evolution and cyclicity. The latter data, integrated with calcareous plankton biostratigraphy, allow a firm and highly resolved chronological framework for the investigated succession. The adopted time framework is reported in Figure 7, which includes the chronostratigraphic scale, geomagnetic polarity time scale (GPTS; Cande & Kent 1992, 1995), Mediterranean calcareous nannofossil biozonation (Rio *et al.* 1990), major planktonic foraminiferal bioevents (after Lourens *et al.* 1996, 2004), reference oxygen isotope curve of benthic Foraminifera from Ocean Drilling Program (ODP) Sites 846 (Shackleton *et al.* 1995*a*,*b*) and 677 (Shackleton *et al.* 1990), and Mediterranean sapropel layers with the i-cycle code (after Lourens *et al.* 1996; Kroon *et al.* 1998). Chronology was derived using the astronomical tuning of Lourens *et al.* (1996, 2004).

Here we report the most significant data collected in the Strongoli area. Calcareous nannofossil biostratigraphy has been established for about 100 samples. Calcareous nannofossil taxonomy and zonation are after Rio *et al.* (1990). Nannofossil quantitative data were collected counting the marker species of *Discoaster* within a total of 20–50 discoasterids; for rarer occurrences, three vertical traverses were analysed. Planktonic and benthic Foraminifera were studied in about 80 samples, 65 of which have been analysed with quantitative methods (at least 300 planktonic and 300 benthic specimens were identified and counted) from the >125 μm fraction

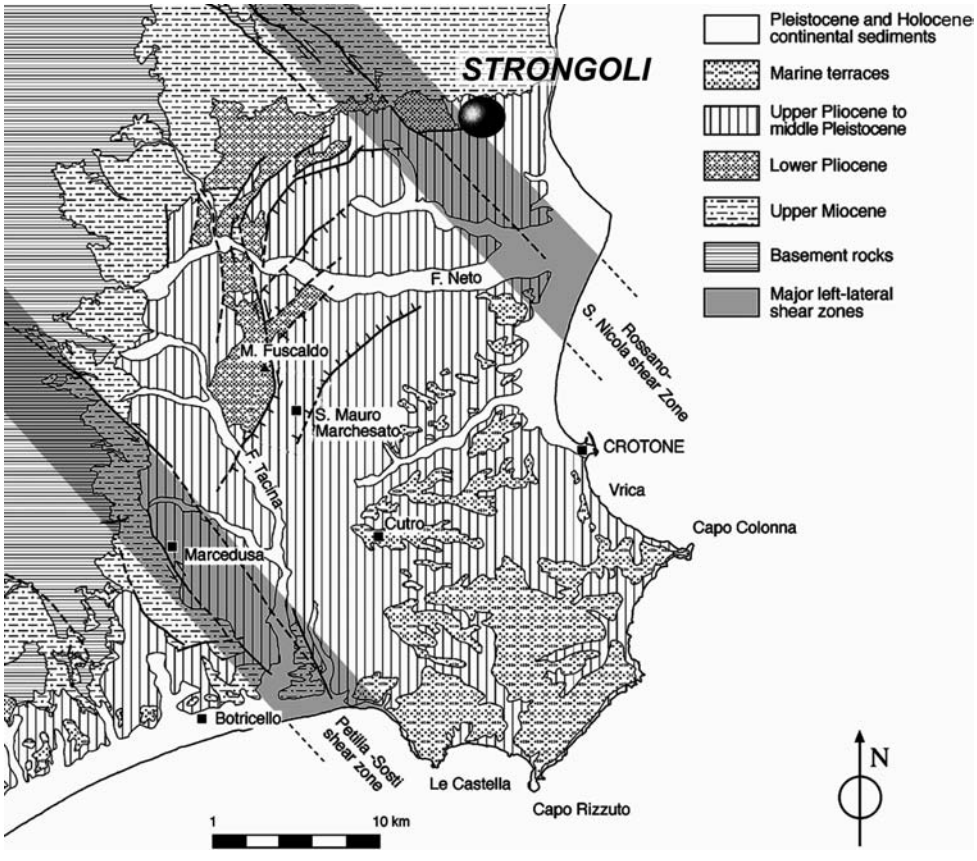

Fig. 2. Simplified geological sketch of the Crotone Basin (modified from Massari *et al*. 2002) and location of study area. Evolution of the Crotone Basin was controlled by two NW-trending crustal shear zones (the Rossano–S. Nicola and Petilia–Sosti Zones).

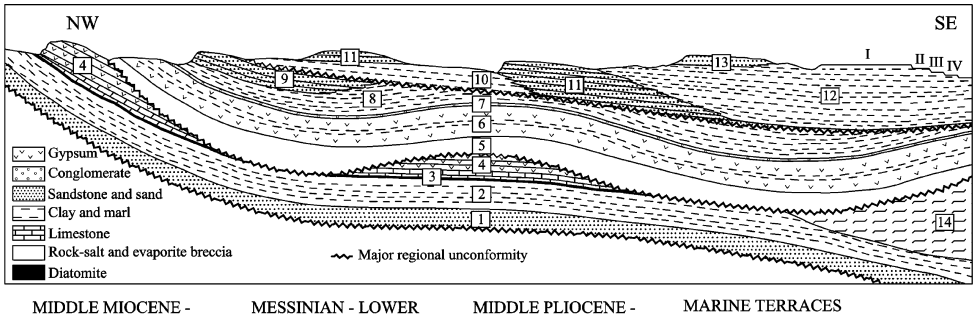

MIDDLE MIOCENE - MESSINIAN CYCLE	MESSINIAN - LOWER PLIOCENE CYCLE	MIDDLE PLIOCENE - PLEISTOCENE CYCLE	MARINE TERRACES (Gliozzi, 1987)
1 S. Nicola Formation	5 Detrital Saline Formation	10 Spartizzo Marly Clay	I Cutro
2 Ponda Marly Clay	6 Upper Evaporite Formation	11 Scandale Sandstone	II S. Leonardo - Campolongo
3 Tripoli Formation	7 Carvane Conglomerate	12 Cutro Marly Clay	III Le Castella - Capo Rizzuto
4 Lower Evaporite Formation	8 Cavalieri Clayey Marl	13 S. Mauro Sandstone	IV Capo Colonna
14 Allochthonous mass	9 Zinga Sandstone		

Fig. 3. Large-scale stratigraphy of the Crotone Basin as outlined by Roda (1964; slightly modified). This paper is focused on the third tectonostratigraphic cycle, particularly on the lower part of the Cutro Marly Clay Unit.

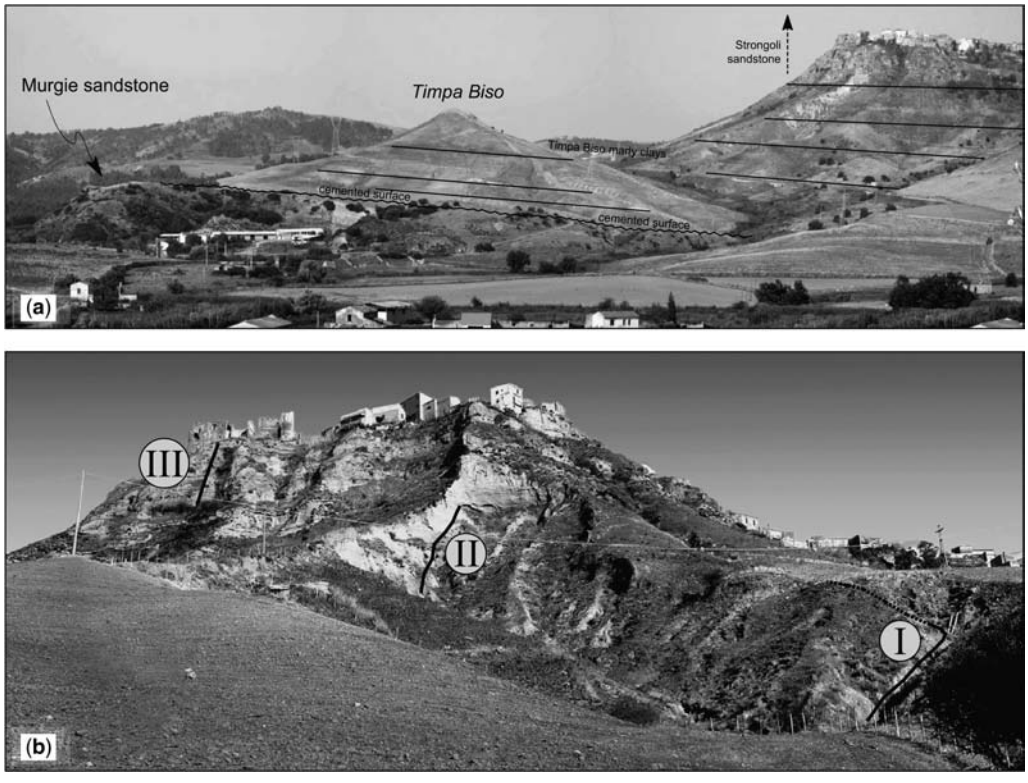

Fig. 4. (**a**) Panoramic view of the Timpa Biso–Strongoli area. Three units can be distinguished: the Murgie sandstone, the Timpa Biso Marly Clay (TBMC) and the Strongoli Sandstone (SS). (**b**) Measured segments of the upward-coarsening Strongoli section. Segments I and II belong to the TBMC; segment III crosses the SS.

of the split residues. Non-quantitative analyses only have been performed on spot samples, for which the relative distribution of foraminifer species is reported in terms of abundant, common or rare occurrence. The complete census dataset is available online as a Supplementary Publication at http://www.geolsoc.org.uk/SUP18250. A hard copy can be obtained from the Society Library. Standard techniques of preparation and microscope analysis have been used. Taxonomy of foraminiferal species is after Kennett & Srinivasan (1983) and Loeblich & Tappan (1988), and palaeoecology is after Sen Gupta (1999, and references therein). Planktonic foraminiferal quantitative data (measured sections only) are presented here in terms of the relative abundance fluctuations of marker species *Globorotalia bononiensis* and *Globorotalia crassaformis* sx (see Fig. 9). By means of the relative distribution of selected planktonic foraminiferal species, a sea surface temperature (SST) proxy model was also reconstructed (Lourens *et al*. 1996), which allows the recognition of cool and warm intervals (Fig. 9). Benthic foraminifers (measured sections only) have been used to construct the benthic foraminifera oxygen index (BFOI) curve, which is largely based on the model proposed by Kaiho (1994; Fig. 9). The planktonic foraminiferal distribution reported by Lourens *et al*. (1996) and Sprovieri *et al*. (1998) has been used as reference (particularly for the correlations of sapropel-like layers). Stable oxygen isotope analyses of 55 samples have been carried out on the planktonic foraminiferal species *Globigerinoides ruber* and the benthic foraminiferal species *Cibicidoides dutemplei*, *Uvigerina peregrina* and *Uvigerina bononiensis*. Analyses were performed by an automatic Finnigan MAT 252 mass spectrometer at the Department of Geology and Geochemistry of Stockholm University. Data are reported in δ notation with respect to the VPDB standard reference; measure precision is about $\pm 0.1‰$. For pollen analysis, we have processed 57 samples. From each sample, 10 g of sediment were treated according to standard acid–alkali procedures followed by heavy liquid separation ($ZnCl_2$ at $d = 2.004$) and ultrasound treatment. A minimum of 120 pollen grains was counted in each sample excluding *Pinus*.

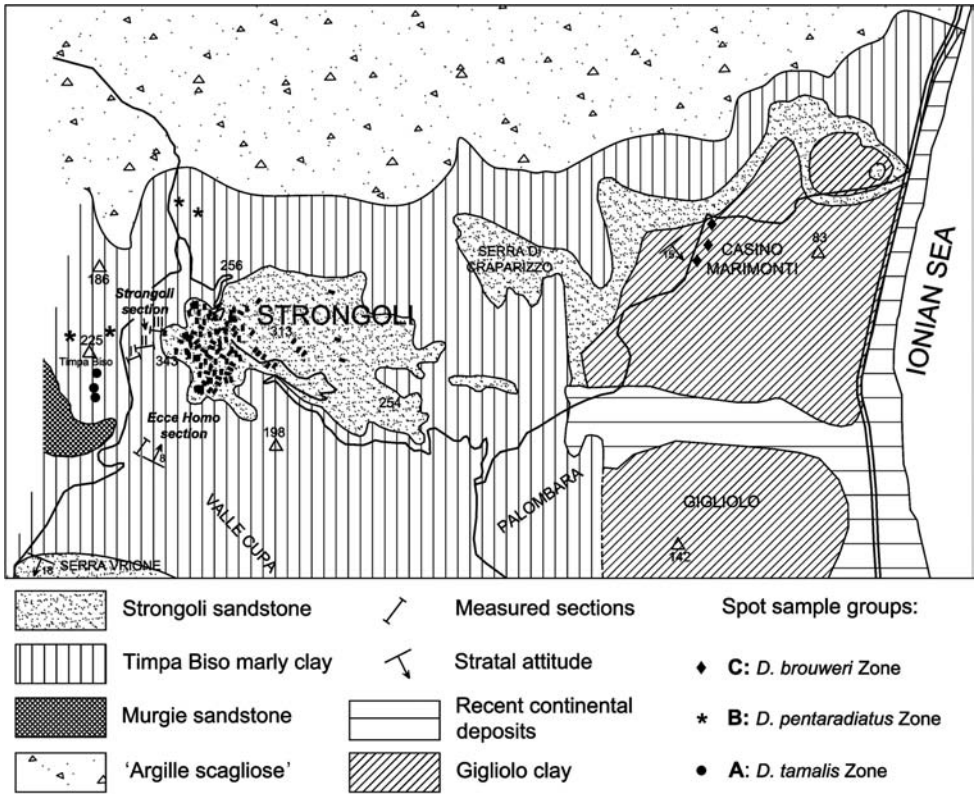

Fig. 5. Simplified geological map of the Strongoli area (modified from Ogniben 1955). Measured sections and principal spot samples are reported.

Ogniben (1955)	**Roda** (1964)
Gigliolo clay	Cutro marly clay
Strongoli sandstone	
Timpa Biso marly clay	
Scandale sandstone	Scandale
Spartizzo marly clay	Spartizzo

Fig. 6. Simplified comparison between the informal terminology proposed by Ogniben (1955) and that of Roda (1964) for subdividing the stratigraphy of the Strongoli area.

Fern and fungal spores and dinoflagellate cysts were not included in the pollen sum.

The Strongoli stratigraphic succession

In the Strongoli area, part of the stratigraphic succession is poorly exposed (Fig. 4). A continuous succession could not be reconstructed, apart from two well-exposed sections (the Ecce Homo and Strongoli sections), which have been sampled in detail (Figs 4a and 9). In contrast, intervening tracts have been spot sampled only (Fig. 5). Although distances between the measured sections might prevent a firm correlation, we reconstructed a composite representative log of the succession by splicing together four major segments (Fig. 8).

The local substrate of the Timpa Biso Marly Clay

The lower part of the TBMC crops out only along the southern flank of the Timpa Biso hill (Figs 4a and 5).

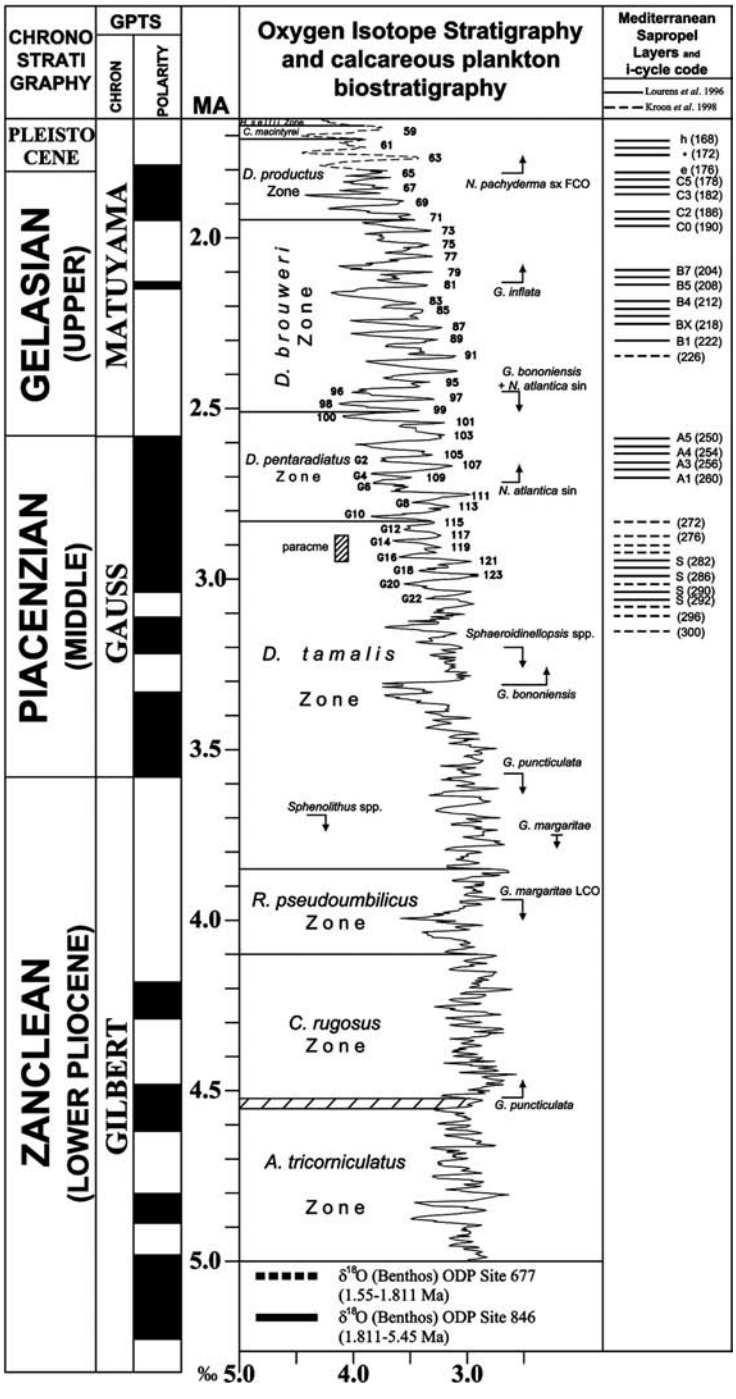

Fig. 7. Adopted time framework. Chronostratigraphic and geomagnetic polarity time scale (GPTS) are after Lourens *et al*. (1996, 2004). Oxygen isotope stratigraphy is after Shackleton *et al*. (1990, 1995*a*,*b*). Calcareous plankton biostratigraphy is after Rio *et al*. (1990), Sprovieri *et al*. (1994, 1998) and Lourens *et al*. (1996, 2004). Mediterranean sapropel layers are after Lourens *et al*. (1996) and Kroon *et al*. (1998). FCO, first common occurrence; LCO, last common occurrence.

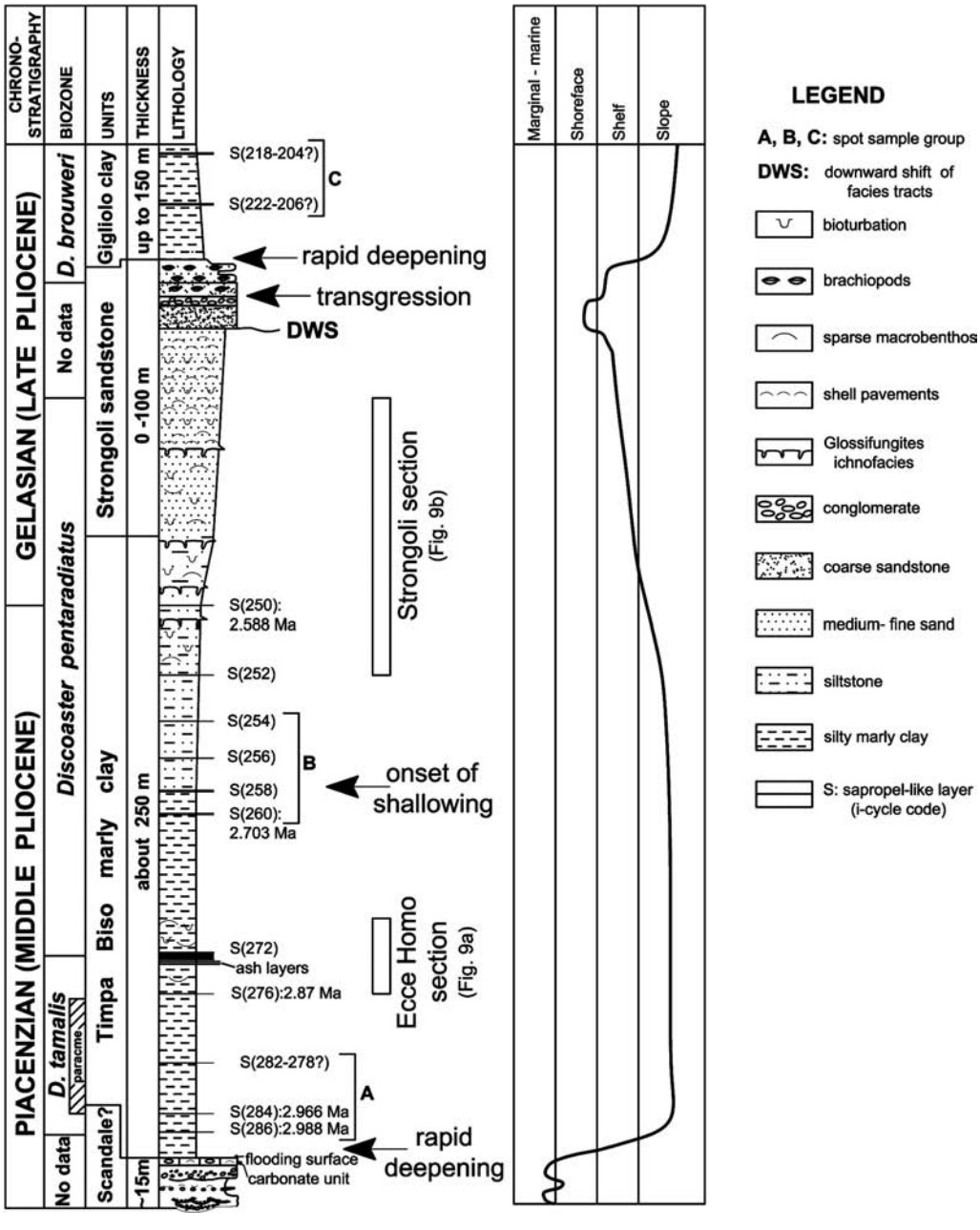

Fig. 8. Simplified log of the Strongoli succession according to the adopted chronological framework. Major stratigraphic events and inferred palaeobathymetry are indicated.

Here, below the TBMC, a sandy–pebbly unit consisting of a number of transgressive–regressive, marginal-marine cycles is present that might correlate with the Spartizzo–Scandale complex (Fig. 8). This unit is discontinuously capped by shallow-marine, highly fossiliferous and tightly cemented sandy and pebbly limestones with *Isognomon* and large pectinids. Immediately above, a thin lag of bored pebbles

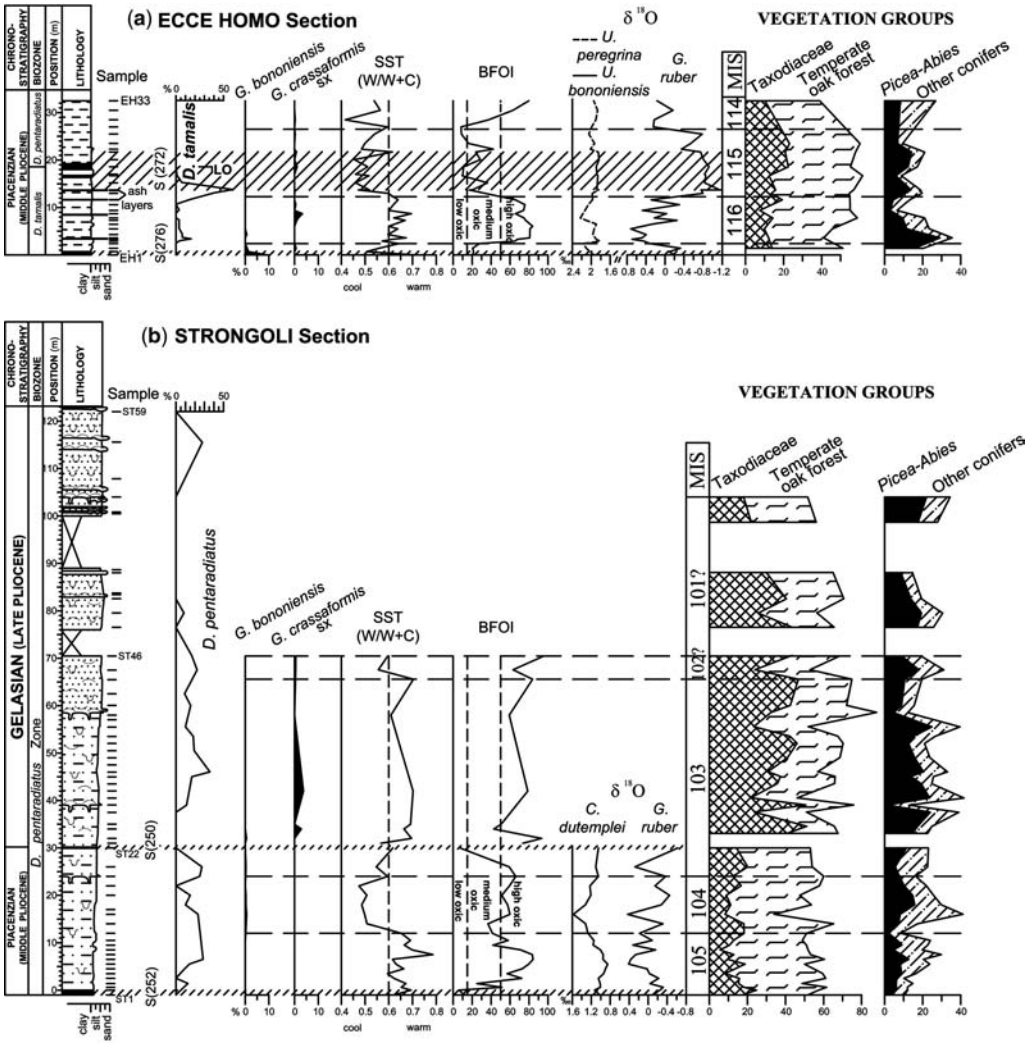

Fig. 9. Palaeoclimatic and biostratigraphic data from the Ecce Homo (**a**) and Strongoli (**b**) sections. Left: stratigraphic log of the sections and distribution of marker nannofossil species in terms of percentage of the total discoasterids assemblage. Middle: data based on foraminiferal assemblages. Distribution of planktonic Foraminifera marker species *Globorotalia bononiensis* and *Globorotalia crassaformis* sx in terms of percentage of the total assemblage. SST, proxy curve of sea surface temperature, i.e. a ratio between 'Warm' (W) and 'Cold' (C) planktonic Foraminifera species: W/(W + C). 'Warm' species are *Globigerinoides* ex gr. *ruber*, *G. obliquus*, *G. sacculifer* gr., *Zeaglobigerina* spp., *Orbulina universa* and *Globorotalia crassaformis*. 'Cold' species are *Globigerina falconensis*, *G. quinqueloba*, *G. glutinata*, *Neogloboquadrina* spp. sx and *Globorotalia scitula* (after Lourens *et al*. 1996). BFOI, Benthic foraminifer oxygen index, i.e. the ratio between 'Oxic' (O) and 'Dysoxic' (D) benthic foraminiferal species: ((O/(O + D)) × 100 (after Kaiho 1994). 'Oxic' species are *Cibicides* spp., *Cibicidoides* spp. *Globocassidulina* spp. *Pyrgo* spp. and *Quinqueloculina* spp. 'Dysoxic' species are *Bolivina* spp., *Bulimina exilis*, *Chilostomella oolina, Fursenkoina schrembersiana*, *Globobulimina* spp., *Stainforthia complanata*, *Stilostomella* spp., *Uvigerina bononiesis* and *U. cylindrical*. Dashed bars indicate low-oxygen intervals. Oxygen isotope data are given in δ notation with respect to the VPDB standard. MIS, correlative Marine Isotope Stages as deduced from oxygen isotope, microfaunal and pollen data. Right: selected vegetation groups with high ecological significance. Relative percentages of pollen taxa are calculated without *Pinus*. Taxodiaceae (*Taxodium* + *Sciadopitys* + *Nyssa*) and temperate forest elements (*Quercus* + other mesothermic broad-leaved trees) are indicative of a warm and humid climate; *Picea* + *Abies* + other conifers (*Tsuga* + *Cedrus*) indicate cool to cold climatic conditions with high precipitation rates.

and cobbles is present, which can be extensively traced laterally in the field as a marker horizon (Figs 4a and 8).

The Timpa Biso Marly Clay: deepening stage

The abrupt transition from the carbonate unit to the overlying outer-shelf and upper slope hemipelagic mudstones (TBMC) suggests a rapid deepening (Fig. 8). The base of the TBMC is not exposed, being generally hidden below a grass cover. The lower part of the TBMC mainly consists of silty marly clay and marly silt with sparse sandy beds, two ashbeds and a number of laminated sapropel-like layers (Figs 8 and 9). The latter usually indicate a palaeodepth in excess of 300 m (as suggested by Rohling & Gieskes 1989).

We spot sampled the lowermost outcrops of the TBMC on the southern side of the Timpa Biso hill (group A, Fig. 5). These samples belong to the *Discoaster tamalis* Zone, the paracme interval of which (extending from Marine Isotope Stage (MIS) 121 to MIS 117, according to Sprovieri *et al*. 1994, 1998) was clearly recognized (Fig. 8). In this sampling area, three sapropel-like laminated layers have been detected in the field (corresponding to samples TB/02/10, TB/02/16-17 and TB/02/23 as coded in the Supplementary Publication 18250 tables; see p. 000). In these layers, siliceous remains are abundant and benthic foraminiferal assemblages are dominated by low-oxygen tolerant genera such as *Bolivina*, *Bulimina* and *Uvigerina* (Sen Gupta 1999, and references therein). Based on their stratigraphic position with respect to the peculiar distribution pattern of *D. tamalis* (before the paracme, Fig. 8) the presence of *Globorotalia bononiensis* and the presence or absence datum of *Globorotalia crassaformis* dx (see Supplementary Publication tables), two of these sapropel-like layers can be confidently correlated with the Mediterranean sapropels i-cycle 286 (2.988 Ma) and i-cycle 284 (about 2.966 Ma). Minor constraints are available for the third sapropel-like layer (Fig. 8), which occurs within the *D. tamalis* paracme interval and thus might correlate with Mediterranean sapropel i-cycle 282 (2.943 Ma), i-cycle 280 (2.921 Ma) or i-cycle 278 (2.900 Ma). The Last Occurrence (LO) of *D. tamalis* (2.83 Ma) has been detected in the middle part of the Ecce Homo section, which belongs to the *Discoaster pentaradiatus* Zone (2.83–2.51 Ma) in its upper part (Fig. 9a). In this section, oxygen isotope analyses, as well as quantitative analyses of the foraminiferal and pollen contents, have been performed (Fig. 9a). Based on the oxygen isotope ratio, two glacial–interglacial cycles have been recognized. Both interglacials are characterized by low-oxygen conditions (dashed bars in Fig. 9a) and very light $\delta^{18}O$ planktonic values (Fig. 9a). Interestingly, the SST curve shows low values during these intervals, mainly because of a frequency drop in the oligotrophic, warmth-demanding planktonic species *Globigerinoides* ex gr. *ruber* and *Zeaglobigerina* spp. (Hemleben *et al.* 1989; Pujol & Vergnaud-Grazzini 1995). Together, these data suggest that $\delta^{18}O$ interglacials in the Ecce Homo section were characterized by eutrophic conditions possibly favoured by increases in freshwater runoff. The lower low-oxygen episode occurs just above the paracme of *D. tamalis*. As *G. bononiensis* is rather abundant (about 10% of the total assemblage; Fig. 9a), this interval might correlate with the Mediterranean sapropel i-cycle 276 (*c*. 2.87 Ma). The LO of *D. tamalis*, which is correlative with interglacial MIS 115/G11 (Fig. 7), has been confidently detected within the upper sapropel-like interval (Fig. 9a). It follows that the latter corresponds to the Mediterranean sapropel i-cycle 272 (2.828 Ma) and, consequently, correlation of glacial intervals below and above with MIS 116/G12 and 114/G10, respectively, is straightforward (Fig. 9a).

Two further laminated sapropel-like layers have been recognized in the spot samples collected between the Ecce Homo and Strongoli sections (group B in Fig. 5, TB/02/5 and ST/03/1-3 as coded in the Supplementary Publication tables), which belong to the *Discoaster pentaradiatus* Zone (Fig. 8). Both these layers are characterized by abundant *G. bononiensis*; however, one is dominated by 'cold' and 'eutrophic' planktonic species, whereas the other is dominated by 'warm' species (see Supplementary Publication tables). These planktonic assemblages closely resemble those reported by Lourens *et al*. (1996) for the Mediterranean sapropels i-cycle 260 (2.703 Ma) and i-cycle 258 (2.679 Ma), respectively.

The shallowing stage: transition from Timpa Biso Marly Clay to Strongoli Sandstone

A shallowing trend begins some tens of metres below the Strongoli section and develops in this section, as clearly indicated by coarsening from clayey silt to fine to medium, highly fossiliferous sand (Fig. 8). Below the Strongoli section, spot samples belonging to the *Discoaster pentaradiatus* Zone have been collected (group B, Fig. 5; KR/03/143 and KR/03/142 in the Supplementary Publication tables), in which benthic foraminiferal assemblages suggest the occurrence of two distinct low-oxygen intervals. The lower one (KR/03/143) is characterized by a planktonic assemblage similar to that described by Lourens *et al*. (1996) for the Mediterranean sapropel i-cycle 256 (*c*. 2.658 Ma), whereas the upper (KR/03/142) is faunistically similar to the Mediterranean sapropel i-cycle 254 (2.632 Ma; Lourens *et al*. 1996).

From the base up to *c*. 83 m, the Strongoli section (Fig. 9b) is composed of silts and fine sands that are thoroughly bioturbated with sparse macrobenthic assemblages dominated by *Turritella*, pectinids, scaphopods, ahermatypic corals and annelids. Four firmground horizons draped by *Neopycnodonte* clumps and marked by *Glossifungites* ichnofacies at 24, 39, 58.5 and 104 m may record minor flooding events. Starting from about 83 m, the dominant sedimentation pattern consists of cyclic alternation of bioturbated fine sands and highly fossiliferous fine to medium sands and sandstones with common pavements and layers of transported shells forming sedimentological concentrations with convex-up and locally nested valves (Fig. 9b). In the upper Strongoli section and above, sediments are either (1) not cemented or poorly cemented, or (2) cemented into some protruding sandstone layers as a result of selective erosion (Figs 8 and 9b). Common plant remains and sedimentological features suggest a direct or lateral link with a prograding, wave- and storm-influenced delta system developing from a prodelta to a delta-front setting.

In the upper part of the Strongoli Sandstone Unit, a sharp transition to fossiliferous coarse shoreface sandstone and fine-grained conglomerate layers that sparsely crop out may indicate a downward shift of the facies tracts (DWS in Fig. 8).

The entire Strongoli section (about 120 m) belongs to the *Discoaster pentaradiatus* Zone (Fig. 9b). In the lower part of the section (0–30 m), oxygen isotopes and both foraminiferal and pollen assemblages document a full glacial interval bracketed by two interglacials (Fig. 9b), in the midst of which two low-oxygen episodes have been recognized (see the BFOI in Fig. 9b). These low-oxygen episodes (which are located at the base of the section and at 30 m level, respectively) can be confidently correlated with the Mediterranean sapropels i-cycle 252 (2.611 Ma) and 250 (2.588 Ma; Figs 8 and 9b). Therefore, it follows that the lower part of the Strongoli section (0–30 m) corresponds to the MIS 105–MIS 103 interval (Figs 7 and 9b). Above, from 30 to 104 m level, foraminiferal assemblages (where available) indicate persisting warm climatic conditions (see the SST curve in Fig. 9b), as also confirmed by a pollen assemblage dominated by warmth-demanding Taxodiaceae (Fig. 9b). Thus, the interval from 30 to 104 m level may correlate with the long MIS 103–101 interglacial complex, during which no severe glacial occurs (Figs 7 and 9b). In fact, we did not detect pollen evidence of the prominent MIS 100–96 glacial complex, which is well documented in Northern Italy as a time of severe glacial conditions (e.g. Marecchia section: Rio *et al.* 1997), although it is not well known from Southern Italy.

Pollen and microfaunal analyses are not feasible in the upper portion of the Strongoli Sandstone because of the unsuitable facies. However, recognition of the interglacial MIS 103–101 complex (Fig. 9b) suggests that the upper part of the SS encompasses at least the glacial MIS 100. Thus, we speculate that the downward shift recognized close to the top of the SS may have been chiefly controlled by glacioeustasy (Fig. 8).

The Gigliolo Clay transgression and abrupt deepening

At the top of the SS, a distinct transgressive sheet is present that consists of highly fossiliferous sandstone and pebbly sandstone separated by a silty layer (Fig. 8). This interval, which is some 5 m thick, is overall very rich in brachiopods with subordinate echinoids, pectinids, ahermatypic corals and bryozoans, which are commonly bored and encrusted. The fossiliferous interval grades very rapidly into deep-water silts and marly clays with sapropel-like layers (namely, the Gigliolo Clay, GC; Fig. 8). The transition is rapid but without discontinuity, thus suggesting that the Strongoli area underwent a dramatic tectonic collapse after SS times. Spot samples have been collected from an exposure of the GC in the eastern part of the Strongoli area (group C, Fig. 5). Nannofossil assemblages indicate that the basal portion of the GC (0–20 m) belongs to the *Discoaster brouweri* Zone (Fig. 8). Moreover, the absence of foraminiferal marker species *Globorotalia bononiensis*, *Globorotalia inflata* and *Neogloboquadrina atlantica* provides evidence that sedimentation of the GC began after the LO of *G. bononiensis* and *N. atlantica* (2.41 Ma) and before the FO of *G. inflata* (2.09 Ma). Based on this biostratigraphic evidence, the sapropel-like layers recognized in the basal GC (KR/03/155–153 and KR/03/144 in the Supplementary Publication tables) are correlatable with the Mediterranean sapropels of cluster B, between 2.3 and 2.1 Ma (Figs 7 and 8).

Discussion

Onset of Roda's (1964) third tectonostratigraphic sequence

According to Roda's interpretation, in the Strongoli area the base of the CMC (that is, the base of the TBMC of Ogniben 1955) would be time equivalent to the base of the marginal marine–continental units laterally developing west of the study area (i.e. the Spartizzo–Scandale complex). The base of these units would also correlate with the beginning of the third tectonostratigraphic cycle of Roda (1964). Here, for the first time, we provide firm evidence that the onset of Roda's (1964) third cycle is

older than 3 Ma because, in the Strongoli area, the basal CMC (i.e. the TBMC) belongs to the upper *D. tamalis* Zone. In this area, the beginning of the third tectonostratigraphic cycle of Roda (1964) is documented by marginal–continental sediments (the Spartizzo–Scandale complex). Deposition of the deep marine CMC began later in the area, after an unresolved time interval corresponding to the deposition of both the sandy and limestone units (which we consider here as part of the Scandale sandstone) that are present below the TBMC (Figs 4a and 8). According to a very rough evaluation, the time elapsed might be very significant. Thus, evidence is provided that in the Strongoli area, the base of the CMC (i.e. the TBMC) is correlative neither with the base of the Spartizzo–Scandale complex, nor strictly with the beginning of Roda's (1964) third tectonostratigraphic cycle.

The interaction of glacioeustasy–tectonics–sediment supply

Our data suggest that a large part of the regression associated with the deposition of the SS is not primarily controlled by glacioeustasy. In fact, it is proposed that (1) most of the shallowing trend from the TBMC to the SS takes place under warm and humid climatic conditions (i.e. fully interglacial; Fig. 9b) that are usually correlative with high sea level, and (2) the total thickness of the regressive portion of the TBMC (some 100 m; Fig. 8) is not large enough to explain a simple terrigenous infill of the former accommodation space (of the order of 200–300 m) without invoking a strong synsedimentary uplift. It follows that the regressive evolution of the TBMC–SS complex was probably largely shaped by tectonics. Likewise, the rapid deepening corresponding to the base of the TBMC can be explained only in terms of accelerated subsidence. Nevertheless, we speculate that the downward shift recognized in the upper SS may reflect a major glacioeustatic event (i.e. the glacial MIS 100). In this case, we would confirm that glacioeustasy may still be readable also in active tectonic settings such as that of the Crotone Basin (i.e. Rio *et al.* 1996; Massari *et al.* 2002) although tectonics and sedimentary supply are still dominant in shaping the large-scale architecture of the stratigraphic record.

The rapid deepening events at the onset of the GC deposition

Above the SS, the GC unit records a dramatic deepening of the Strongoli area in the *Discoaster brouweri* Zone, between 2.3 and 2.1 Ma. In the interpretation of Ogniben (1955), the beginning of the GC deposition is correlative with the so-called 'Calabrian transgression' *Auctorum* (e.g. Gignoux 1913; Ruggeri & Selli 1948; Selli 1949). Apparently, this event is not just local in scope because, beginning from Late Pliocene–Early Pleistocene times, a thick succession of deep-marine sediments is widespread over the entire Crotone Basin. Here, we provide tight chronological framing that this regional event began in Late Pliocene times, and thus, the so-called 'Calabrian transgression' is not Pleistocene in age (at least in the Crotone Basin area), as suggested by previous studies (e.g. Gignoux 1913; Ruggeri & Selli 1948; Selli 1949; Ogniben 1955). Moreover, we demonstrate that the so-called 'Calabrian transgression' occurs mainly in response to the tectonic collapse of the entire Crotone Basin rather than because of glacioeustasy.

The regional geological framework

Van Dijk (1991, 1992, 1994) and Van Dijk *et al.* (1998) subdivided the tectonostratigraphic development of the Crotone Basin into four stages: (1) a Serravallian–early Messinian stage of progressive enlargement of the basin, closed by a major intra-Messinian transpressional tectonic event; (2) a mid-Messinian–Early Pliocene stage characterized by intense faulting overprinted by the Messinian salinity crisis, and closed by a major Mid-Pliocene compressional phase responsible for basin closure; (3) a Late Pliocene–Early Pleistocene stage, characterized by pulsating onlap, and later interpreted (Van Dijk & Scheepers 1995) to be closed by a regional Mid-Pleistocene contraction phase accompanied by oroclinal-type rotations, transpressions and basin inversions; (4) a Mid-Pleistocene–Recent stage, characterized by strong vertical movements. Stress analyses revealed a pattern of overall tension, with three major phases of subsidence and basin opening in late Tortonian, Early Pliocene and Late Pliocene times, interrupted by short periods of compressional deformation in the Mid-Pliocene and Mid-Pleistocene. The extensional stages would correlate with long episodes of rollback, translation of the Calabrian lithosphere to the SE, attributed to gravitational displacement and spreading in the Tyrrhenian back-arc area. Phases of cessation of spreading in the back-arc basin would have coincided with interruption of slab migration. This would have resulted in short pulses of regional compression caused by the movement of the African Plate relative to the European Plate, which generated a component of NE-directed translation of the Calabrian block (Van Dijk 1992).

Focusing specifically on the Pliocene evolution, a strongly extensional–transtensional regime and high subsidence rate dominated in the Crotone Basin from the late Messinian and especially during the Early Pliocene. This regime is recorded by

spectacular listric normal growth faults in the Lower Pliocene succession (Van Dijk 1991; Moretti 1993; Zecchin *et al.* 2004). As already noted, a contractional phase possibly at the end of the Early Pliocene can be documented throughout the Crotone Basin (Roda 1964; Van Dijk 1991, 1994; Zecchin *et al.* 2004). Transpressional and compressional effects can be recognized throughout the basin and are recorded in its northern part by a major erosional and angular unconformity corresponding to the base of Roda's (1964) third tectonostratigraphic cycle.

This contraction phase should coincide with a major phase of shortening, where upper Messinian and Lower Pliocene deposits of both internal and external chain domains were incorporated in the thrust belt and unconformably covered by sediments of the *Globorotalia puncticulata* Zone of Sprovieri (1992) (Patacca *et al.* 1990; Sartori 1990). In the Crotone Basin, data collected so far are not sufficient to firmly constrain this event in time. However, we speculate that the base of the third tectonostratigraphic cycle of Roda (1964) might fully, or at least partly, represent the regional response of the Calabrian forearc to the *G. puncticulata* event. Unfortunately, as stated above, in the Strongoli area the base of the third cycle of Roda (1964) is documented by shallow-water sediments that are not amenable to biochronological studies. Further investigations are needed on the Mid-Pliocene offshore sediments of the Crotone Basin, where the base of Roda's third cycle is likely to be represented by an uninterrupted stack of deep-marine clays belonging to the CMC.

A second, rapid acceleration of subsidence occurred during Late Pliocene times (the GC event). According to Ogniben (1955), this event corresponds to the so-called 'Calabrian transgression' reported by various workers as a supra-regional event recognized in several localities of the Italian peninsula (Gignoux 1913; Ruggeri & Selli 1948; Selli 1949). This event is well documented in the northeastern marginal part of the Crotone Basin, where deep-marine sediments abruptly were overlain on a shallow-marine substrate. Collapse was then followed by continuing high subsidence rates throughout the latest Pliocene and Early Pleistocene, as shown by the exceptionally thick dominantly hemipelagic succession of this age in the Crotone Basin.

The connections with back-arc events in the Tyrrhenian Sea

As currently known, the migration of the Calabrian arc was characterized most of the time by an upper plate velocity slower than the rollback velocity, so that extension in the upper plate and opening of back-arc basins kept pace with the trench retreat (Malinverno & Ryan 1986). The geodynamic frame leading to rapid retrograde motion of a subducting plate and concurrent opening of a back-arc basin is typically that of a subduction zone that has become narrow in the along-trench direction after a process of slab break-off (Dvorkin *et al.* 1993; Gvirtzman & Nur 1999, 2001; Faccenna *et al.* 2001*a*,*b*, 2004).

Rollback velocity was much greater in the southern Tyrrhenian Basin (5–6 cm a^{-1} according to Faccenna *et al.* 2004; 6–10 cm a^{-1} according to Rosenbaum & Lister 2004), than in the northern Tyrrhenian Basin, where it did not exceed 2 cm a^{-1}, because in the southern area the subducting lithosphere (the Ionian downgoing slab) remained oceanic until the present day, whereas in the northern area rollback slackened as a result of buoyancy of the subducting continental lithosphere (Dercourt *et al.* 1986; Malinverno & Ryan 1986; Patacca *et al.* 1990; Royden 1993; Rosenbaum & Lister 2004). Several researchers (e.g. Patacca *et al.* 1990; Rosenbaum & Lister 2004, and references therein) have argued that differential rates of extension between the northern and southern Tyrrhenian Sea may have been accommodated by the activation of two major crustal shear zones allowing the rapid southeastward migration of the Calabrian block. Slab tear led to the formation of a narrow subducting slab beneath the Ionian Sea whose width is estimated at *c.* 200 km. Lateral mantle flow around the slab flanks was accompanied by their large-scale rotation, leading to oroclinal bending of the arc (Faccenna *et al.* 2004; Rosenbaum & Lister 2004).

Oceanization in the southern Tyrrhenian Basin took place through discrete jumps with southeastward polarity. Rifting and spreading episodes first generated the Vavilov Basin, then the Marsili Basin. Kastens *et al.* (1988) concluded that formation of basaltic crust in the Vavilov Basin may have began during the late Miocene, and the process was certainly widespread by the Early Pliocene. Biostratigraphic data for the oldest cored sediments overlying the basaltic basement of Marsili Basin have been obtained from ODP site 650 (Kastens *et al.* 1987). The position of the drill site was chosen in a location (near the western rim of the basin) ensuring that the basement age is probably the oldest in the basin (Kastens *et al.* 1987). The cored nannofossil ooze has been attributed to the terminal part of the *Discoaster brouweri* Zone because of the presence of the zonal marker species associated with *G. inflata* (i.e. between 2.1 and 1.95 Ma, according to the new chronology of Lourens *et al.* 1996). This is a minimum age for the opening of the Marsili Basin, as it may be assumed that the spreading event initiated and developed somewhat before the age of the overlying sediments.

Conclusions

Data presented in this paper provide a new chronological control on the geological evolution of a

marginal although critical sector of the Crotone Basin. For the first time, a good chronology is available both for establishing a minimum age for the third tectonostratigraphic cycle of Roda (1964) and for constraining the age of the so-called 'Calabrian transgression' *Auctorum.* This chronology also provides time controls that are regional and supraregional in scope when compared with the overall evolution of the Calabrian back-arc (i.e. the Tyrrhenian Basin; Fig. 1). Our data suggest that the Gigliolo Clay collapse event in the forearc Crotone Basin is very close in time to the rifting associated with the oceanization of the Marsili Basin, which resulted in a strong acceleration in the regional subsidence. Thus, it is tempting to infer that this event in the Tyrrhenian Basin correlates with the beginning of the deposition of the exceptionally thick Late Pliocene and Early Pleistocene succession of deep-marine sediments that are exposed in the Crotone Basin (i.e. the Cutro Marly Clay *pro parte*).

This research has been funded by the University of Padova (Progetto Giovani Ricercatori 2003) to L. Capraro and by MIUR (PRIN 2001) to F. Massari. We thank J. Backman, P. Torssander and K. Hajnal for help in isotope analysis. Thanks go to R. Sprovieri and C. Turner for their constructive reviews.

References

CANDE, S. C. & KENT, D. V. 1992. A new geomagnetic polarity time scale for the Late Cretaceous and Cenozoic. *Journal of Geophysical Research*, **97**, 13917–13951.

CANDE, S. C. & KENT, D. V. 1995. Revised calibration of the geomagnetic polarity time scale for the Late Cretaceous and Cenozoic. *Journal of Geophysical Research*, **100**, 6093–6095.

DERCOURT, J., ZONENSHAIN, L. P., RICOU, L.-E., *ET AL*. 1986. Geological evolution of the Tethys belt from the Atlantic to the Pamirs since the Lias. *Tectonophysics*, **123**, 241–315.

DVORKIN, J., NUR, A., MAVKO, G. & BEN-AVRAHAM, Z. 1993. Narrow subducting slabs and the origin of backarc basins. *Tectonophysics*, **227**, 63–79.

FACCENNA, C., BECKER, T. W., LUCENTE, F. P., JOLIVET, L. & ROSSETTI, F. 2001*a*. History of subduction and back-arc extension in the Central Mediterranean. *Geophysical Journal International*, **145**, 809–820.

FACCENNA, C., FUNICIELLO, F., GIARDINI, D. & LUCENTE, F. P. 2001*b*. Episodic back-arc extension during restricted mantle convection in the Central Mediterranean. *Earth and Planetary Science Letters*, **187**, 105–116.

FACCENNA, C., PIROMALLO, C., CRESPO-BLANC, A., JOLIVET, L. & ROSSETTI, F. 2004. Lateral slab deformation and the origin of the western Mediterranean arcs. *Tectonics*, **23**, TC1012, doi:10.1029/2002TC001488.

GIGNOUX, M. 1913. *Les formations marines pliocènes et quaternaires de l'Italie du Sud et de la Sicilie*. Annales de l'Université de Lyon, Nouvelle Série 1, **36**.

GLIOZZI, E. 1987. I terrazzi del Pleistocene superiore della penisola di Crotone (Calabria). *Geologica Romana,* **26**, 17–79.

GVIRTZMAN, Z. & NUR, A. 1999. Plate detachment, asthenosphere upwelling, and topography across subduction zones. *Geology*, **27**, 563–566.

GVIRZTMAN, Z. & NUR, A. 2001. Residual topography, lithospheric structure and sunken slabs in the central Mediterranean. *Earth and Planetary Science Letters*, **187**, 117–130.

HEMLEBEN, C, SPINDLER, M. & ANDERSON, O. R. 1989. *Modern Planktonic Foraminifera*. Springer, Berlin.

KAIHO, K. 1994. Benthic foraminiferal dissolved-oxygen index and dissolved-oxygen levels in the modern ocean. *Geology*, **22**, 719–722.

KASTENS, K. A., MASCLE, J., AUROUX, C., *ET AL*. 1987. Site 650: Marsili Basin. *In*: *Proceedings of the Ocean Drilling Program, Initial Reports*, 107, Ocean Drilling Program, College Station, TX, 129–170.

KASTENS, K. A., MASCLE, J., AUROUX, C., *ET AL*. 1988. ODP Leg 107 in the Tyrrhenian Sea: insights into passive margin and back-arc basin evolution. *Geological Society of America Bulletin*, **100**, 1140–1156.

KENNETT, J. P. & SRINIVASAN, M. S. 1983. *Neogene Planktonic Foraminifera. A Phylogenetic Atlas*. Hutchinson & Ross, Stroudsburg, PA.

KROON, D., ALEXANDER, I., LITTLE, M., LOURENS, L. J., MATTHEWSON, A., ROBERTSON, A. H. F. & SAKAMOTO, T. 1998. Oxygen isotope and sapropel stratigraphy in the Eastern Mediterranean during the last 3.2 million years. *In*: ROBERTSON, A. H. F., EMEIS, K.-C., RICHTER, C. & CAMERLENGHI, A. (eds) *Proceedings of the Ocean Drilling Program, Scientific Results, 160,* Ocean Drilling Program, College Station, TX, 181–189.

LOEBLICH, A. R. & TAPPAN, H. 1988. *Foraminiferal Genera and their Classification*. Van Nostrand Reinhold, New York.

LOURENS, L. J., ANTONARAKOU, A., HILGEN, F. J., VAN HOOF, A. A. M., VERGNAUD-GRAZZINI, C. & ZACHARIASSE, W. J. 1996. Evaluation of the Plio-Pleistocene astronomical timescale. *Paleoceanography*, **11**, 391–413.

LOURENS, L. J., HILGEN, F. J., LASKAR, J., SHACKLETON, N. J. & WILSON, D. 2004. The Neogene Period. *In*: GRADSTEIN, F., OGG, J. & SMITH, A (eds) *A Geologic Time Scale 2004*. Cambridge University Press, Cambridge, 409–440.

MALINVERNO, A. & RYAN, W. B. F. 1986. Extension on the Tyrrhenian Sea and shortening in the Apennines as result of arc migration driven by sinking of the lithosphere. *Tectonics*, **5**, 227–245.

MASSARI, F., RIO, D., SGAVETTI, M., *ET AL*. 2002. Interplay between tectonics and glacio-eustacy: Pleistocene succession of the Crotone basin, Calabria (southern Italy). *Geological Society of America Bulletin*, **114**, 1183–1209.

MORETTI, A. 1993. Note sull'evoluzione tettono-stratigrafica del bacino crotonese dopo la fine del Miocene. *Bollettino della Società Geologica Italiana*, **112**, 845–867.

OGNIBEN, L. 1955. Le argille scagliose del Crotonese. *Memorie e Note dell'Istituto di Geologia Applicata di Napoli*, **6**, 1–72.

PATACCA, E., SARTORI, R. & SCANDONE, P. 1990. Tyrrhenian basin and Apenninic arcs: kinematic relations since Late Tortonian times. *Memorie della Società Geologica Italiana*, **45**, 425–451.

PUJOL, C. & VERGNAUD-GRAZZINI, C. 1995. Distribution patterns of live planktic foraminifers as related to regional hydrography and productive systems on the Mediterranean Sea. *Marine Micropaleontology*, **25**, 187–217.

RIO, D., RAFFI, I. & VILLA, G., 1990. Pliocene–Pleistocene calcareous nannofossil distribution patterns in the Western Mediterranean. *In*: KASTENS, K. A., MASCLE, J., *ET AL.* (eds) *Proceedings of the Ocean Drilling Program, Scientific Results, 107*. Ocean Drilling Program, College Station, TX, 513–533.

RIO, D., CHANNELL, J. E. T., MASSARI, F., POLI, M. S., SGAVETTI, M., D'ALESSANDRO, A. & PROSSER, G. 1996. Reading Pleistocene eustasy in a tectonically active siliciclastic shelf setting (Crotone peninsula, southern Italy). *Geology*, **24**, 743–746.

RIO, D., CHANNELL, J. E. T., BERTOLDI, R., *ET AL.* 1997. Pliocene sapropels in the northern Adriatic area: chronology and paleoenvironmental significance. *Palaeogeography, Palaeoclimatology, Palaeoecology*, **135**, 1–25.

RODA, C. 1964. Distribuzione e facies dei sedimenti Neogenici del Bacino Crotonese. *Geologica Romana*, **3**, 319–366.

ROHLING, E. J. & GIESKES, W. W. C. 1989. Late Quaternary changes in Mediterranean intermediate water density and formation rate. *Paleoceanography*, **4**, 531–545.

ROSENBAUM, G. S. & LISTER, G. 2004. Neogene and Quaternary rollback evolution of the Tyrrhenian Sea, the Apennines, and the Sicilian Maghrebides. *Tectonics*, **23**, TC1013, doi: 10.1029/2003TC001518.

ROYDEN, L. H. 1993. The tectonic expression of slab pull at continental convergent boundaries. *Tectonics*, **12**, 303–325.

RUGGERI, G. & SELLI, R. 1948. Il Pliocene ed il Postpliocene dell'Emilia. *Giornale di Geologia*, **20**, 1–14.

SARTORI, R. 1990. The main results of ODP Leg 107 in the frame of Neogene to Recent geology of perityrrhenian areas. *In*: KASTENS, K. A., MASCLE, J., *ET AL.* (eds) *Proceedings of the Ocean Drilling Program, Scientific Results, 107*. Ocean Drilling Program, College Station, TX, 715–730.

SELLI, R. 1949. Le conoscenze geologiche sul quaternario gassifero del Polesine e del Ferrarese settentrionale. *Atti VI Convegno Nazionale Metano*, 515–535.

SEN GUPTA, B. K. (ed.) 1999. *Modern Foraminifera*. Kluwer, Dordrecht.

SHACKLETON, N. J., BERGER, A. & PELTIER, W. R. 1990. An alternative astronomical calibration of the lower Pleistocene timescale based on ODP site 677. *Transactions of the Royal Society of Edinburgh*, **81**, 251–261.

SHACKLETON, N. J., CROWHURST, S., HAGELBERG, T., PISIAS, N. G. & SCHNEIDER, D. A. 1995*a*. A new late Neogene time scale: application to Leg 138 sites. *In*: PISIAS, N. G., MAYER, L. A. (eds) *Proceedings of the Ocean Drilling Program, Scientific Results, 138*. Ocean Drilling Program, College Station, TX, 73–101.

SHACKLETON, N. J., HALL, M. A. & PATE, D. 1995*b*. Pliocene stable isotope stratigraphy of Site 846. *In*: PISIAS, N. G., MAYER, L. A. (eds) *Proceedings of the Ocean Drilling Program, Scientific Results, 138*. Ocean Drilling Program, College Station, TX, 337–355.

SPROVIERI, R. 1992. Mediterranean Pliocene biochronology: a high resolution record based on quantitative planktonic foraminifera distribution. *Rivista Italiana di Paleontologia e Stratigrafia*, **6**, 61–100.

SPROVIERI, R., DI STEFANO, E., RIGGI, A. & BUSALACCHI, P. 1994. La sezione intra-pliocenica di Gibil-Gabel (Caltanisetta, Sicilia centrale): un esercizio di biostratigrafia ad alta risoluzione. *Bollettino della Società Paleontologica Italiana*, **33**, 289–298.

SPROVIERI, R., DI STEFANO, E., HOWELL, M., SAKAMOTO, T., DI STEFANO, A. & MARINO, M. 1998. Integrated calcareous plankton biostratigraphy and cyclostratigraphy at Site 964. *In*: ROBERTSON, A. H. F., EMEIS, K.-C., RICHTER, C. & CAMERLENGHI, A. (eds) *Proceedings of the Ocean Drilling Program, Scientific Results, 160*. Ocean Drilling Program, College Station, TX, 155–166.

VAN DIJK, J. P. 1991. Basin dynamics and sequence stratigraphy in the Calabrian Arc (Central Mediterranean); records and pathways of the Crotone Basin. *Geologie en Mijnbouw*, **70**, 187–201.

VAN DIJK, J. 1992. *Late Neogene fore-arc basin evolution in the Calabrian Arc (central Mediterranean); tectonic sequence stratigraphy and dynamic geohistory. With special reference to the geology of Central Calabria*. Geologica Ultraiectina, **92**.

VAN DIJK, J. P. 1994. Late Neogene kinematics of intra-arc oblique shear-zone: the Petilia–Rizzuto fault zone (Calabrian Arc, Central Mediterranean). *Tectonics*, **13**, 1201–1230.

VAN DIJK, J. P. & OKKES, M. 1991. Neogene tectonostratigraphy and kinematics of Calabrian basins; implications for the geodynamics of the Central Mediterranean. *Tectonophysics*, **196**, 23–60.

VAN DIJK, J. P. & SCHEEPERS, P. J. J. 1995. Neotectonic rotations in the Calabrian Arc: implications for a Pliocene–Recent geodynamic scenario for the Central Mediterranean. *Earth-Science Reviews*, **39**, 207–246.

VAN DIJK, J. P., BARBERIS, A., CANTARELLA, G., MASSA, E. & PESCATORI, L. 1998. Central Mediterranean Messinian basin evolution: tectono-eustasy or eustato-tectonics? *Annales Tectonicae*, **12**, 7–27.

ZECCHIN, M., MASSARI, F., MELLERE, D. & PROSSER, G. 2004. Anatomy and evolution of a Mediterranean-type fault bounded basin: the Lower Pliocene of the northern Crotone Basin (Southern Italy). *Basin Research*, **16**, 117–143.